17th World Conference on Earthquake Engineering, 17WCEE
Sendai, Japan - September 13th to 18th 2020

Possible Mechanisms of Generating Velocity Pulses Observed on the Nishihara Village during the 2016 Kumamoto Earthquake (Mj 7.3)

K. Tsuda[1)]

[(1)] *Researcher, Institute of Technology, Shimizu Corporation, kenichi.tsuda@shimz.co.jp*

Abstract

Observed earthquake ground motions are influenced by three factors: the source process, seismic wave propagation, and surface geology. Thus, understanding and properly modeling each factor is very important for simulating ground motions of future earthquakes. The ground motions of recent hazardous earthquakes, such as the 2016 Kumamoto, Japan, earthquake (Mj 7.3), observed very close to the fault have provided new evidence that the source process plays an important role in determining the ground motion configuration and suggests that physical considerations are critical. Ground motions produced by the 2016 Kumamoto earthquake, for example, had periods of more than 1 s and were larger even than those produced by the 1995 Kobe, Japan, earthquake. Therefore, it is preferable to use a physics-based dynamic source model to model the source process. On the other hand, the direct usage of the dynamic source model into ground motion simulation is sometimes difficult due to the uncertainty especially to the initial stress or frictional conditions for the simulation. The accumulation of recent studies based on the experimental results could bring some insights to setting the initial conditions of stress and frictional parameters. In this study, we have applied the dynamic model to the ground motion simulation for the near-fault motions. The simulation is based on the spectral element method (Galvez et al [1]), which the modification of the formulation can lead to the more efficient calculation than conventional finite element method. We have assumed the three SMGA (Strong Motion Generation Area) on the fault plane referred to the model by Satoh [2]. We explored the conditions of initial parameters, such as the location of SMGA, frictional parameters, stress parameters to investigate the conditions to generate the velocity pulses on the near fault motions, such as the observed records at the Nishihara Village during the 2016 Kumamoto Earthquake.

Keywords: Dynamic Model, Near-Fault Ground Motion, Spectral Element Method, 2016 Kuamamoto Earthquake, Velocity Pulse

1. Introduction

The ground motions recorded on the site very close to the fault (near-fault) sometimes accompany velocity pulse with huge amplitude. This pulse-like shape is considered as the very critical for the structures features on the waveform modeling in structural engineering. Since such seismic waves with predominat period around 1 to 2 sec, its predominant period of the lower level building, modeling such waves are very crucial to the hazard mitigation as Koketsu [3] pointed out the importance of these pulse-shaped seismic waves. Since then, the development of the strong motion arraies brought such observations with pulse shape seismic waves such as from earthquakes, mainly inland crustal earthquake. These seismic arraies have gotten the observations for such pulse-like shapes of ground motions such as the 2002 Denali earthquake in Alaska (e.g., Dunhum and Archuleta [4]), recent 2016 Kaikoura earthquake in New Zealand (e.g., Ando and Kaneko[5]) and 2016 Kumamoto earthquake (e.g., Asano and Iwata [6]). For example, waveforms recorded during the mainshock of the 2016 Kumamoto earthquake (M_J 7.3) at Nishihara Village, 0.6 km from the fault (Furumura [7]), are shown in Fig. 1. This earthquake followed a foreshock (M_J 6.4) that occurred two days before the mainshock and generated very large ground motions at nearby fault stations, such as the Mashiki KiK-net seismograph station and Nishihara village, where the maximum intensity level (VII) on the Japan Meteorological Agency (JMA) Seismic Intensity Scale was observed. In addition, distinct velocity pulses with a period of more than 1 s, unusual for an inland crustal earthquake (Furumura [7]), were recognized in the fault-parallel component of the observed seismic waveforms, for example, at Nishihara village shown in Fig. 1. To understand the generation mechanism of such strong near-fault ground motions, it is necessary to

use a physics-based dynamic source model to model the source process. These observations might mainly reflect the source process of the Kumamoto earthquake itself. Some studies have used waveform inversion to infer the source process of the Kumamoto earthquake, but subsequent forward modeling did not reproduce these waveform features (e.g., Asano and Iwata, [6]). Therefore, it is essential to understand the source process that can generate these ground motions. Furthermore, these features of ground motions very close to the fault should be considered when modeling the source processes of possible future earthquakes.

In this study, we have tried to make discussions about the possible mechanism to generate such pulses like the one observed on Nishihara Village. Then, the possibility to generate similar pulses on other active fault in Japan based on the dynamic propagation of the rupture in also discussed.

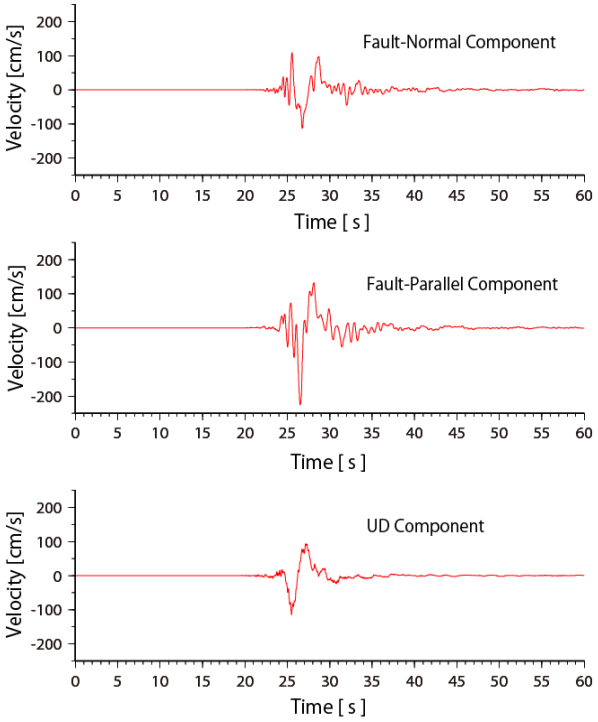

Fig.1 Observed waveforms at Nishihsra Village during mainshock of the Kumamoto earthquake (Filetered 0.1-10.0 Hz, strike is assumed to be 235N, Asano and Iwata [6])

2. Simulation Procedure

2.1 Model Setting

The source process of the 2016 Kumamoto earthquake has been inferred by inversion of observed waveforms, including teleseismic data (e.g., Yue et al., [8]), strong motion data (e.g., Asano and Iwata, [6]), and both teleseismic and strong motion data (e.g., Kobayashi et al., [9]). Characterized source models have also been proposed (e.g., Satoh, [2], Hikima [10]) for this earthquake to reproduce near-fault ground motions over a broad frequency band. Such characterized models are often used for engineering purposes to observed records and to calculate the ground motions of future earthquakes. We adopted the characterized model of Satoh [2], who identified four strong motion generation areas (SMGAs), one along the Hinagu segment and three along the Futagawa segment of the Kumamoto earthquake fault (Fig. 2). On the basis of the Satoh [2] model, Tsuda and Kawabe [11] argued that even though the Hinagu segment (e.g., Fig 2(a)) contributes to the accumulation of total seismic moment, its contribution to ground motion at sites such as the Mashiki KiK-net site is very small. Because the objective of this study was to develop a methodology for simulating ground motions, not to reproduce the observed features of the Kumamoto earthquake, we consider here only the three SMGAs on the Futagawa segment. The geometry of these SMGAs is shown in Fig. 2(b). We set a 4

km x 4 km nucleation zone on the downdip side of SMGA3 to satisfy the conditions for rupture propagation (Galis et al., [12]).

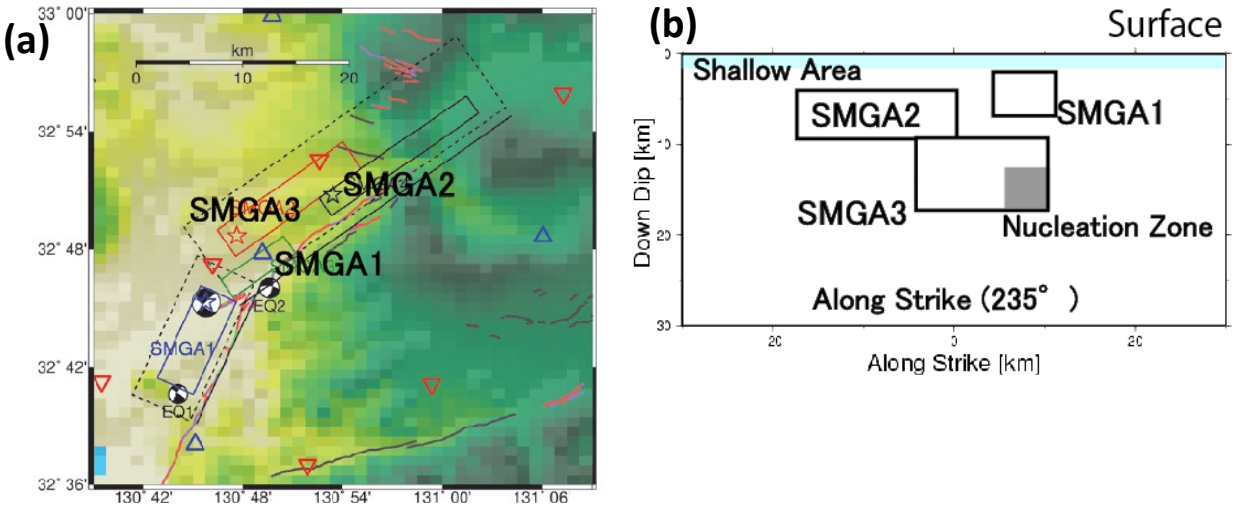

Fig. 2 Characterized source model of the 2016 Kumamoto earthquake (Modified from Satoh [2]). The red circles correspond to the sites where we show the simulated ground motions later. The upper and lower triangles donate the sites of strong motion sites managed by local government and KiK-net sites, respectively (a). Model geometry of the strong motion generation areas and nucleation zone on the fault plane (b)

2.2 Simulation Conditions

For the constitutive relation that determines how faulting proceeds in our simulations, we assumed a slip-weakening relation in which shear stress varies as a function of slip distance (e.g., Ida, [13], Fig. 3). To specify this relation, we set five initial parameter values: normal stress, shear stress, the static coefficient, the dynamic coefficient, and slip-weakening distance (Dc).

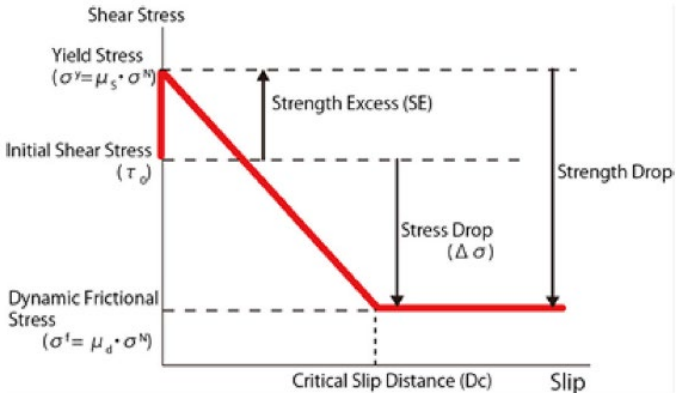

Fig. 3 Slip-weakening relation assumed as the constitutive relation (Ida, 1972)

We imposed these parameters on the fault plane by referring to previous studies as follows. The distributions of the stress parameters strength excess (SE), stress drop (Δσ), and Dc assumed for each area (Table 1) are shown in Fig. 4. So that the rupture propagation would be physically reasonable, we assumed that the stress ratio S (= SE / Δσ) was 1 in each SMGA to suppress rupture velocity. We also assumed depth-dependent normal and shear stress values in the shallow area (see Fig. 2(b)). Near-surface stress conditions

can be modeled in several ways, for example, as velocity strengthening, reflecting a cohesive force (e.g., Aochi, [14]), or as an area of negative stress drop. However, for simplicity, we assumed that shear and normal stresses were linearly distributed and approached zero near the surface. To set Dc, we referred to Urata et al. [15], who dynamically simulated the mainshock of the Kumamoto earthquake by the boundary integral method. After setting these parameters to specify the slip-weakening relation, we simulated the rupture propagation by the spectral element method.

For simplicity, we assumed a homogeneous material (Vp = 5.91 km/s, Vs = 3.41 km/s, ρ = 2700 kg/m^3) without attenuation (Q = infinity) and a planar fault with a dip of 65° (Asano and Iwata, [6]). Thus, the effective frequency for the simulation was below 2.5 Hz. The assumed focal mechanism is right-lateral strike slip like main shock of the Kumamoto earthquake.

Table 1 Assumed source parameters for each area (e.g., Fig 2(b))

Area Name (Size)	Stress Drop [MPa]	Strength Excess [MPa]	Dc [m]
SMGA1 (7.2km x 4.8km)	10	10	0.5
SMGA2 (16.8km x 4.8km)	10	10	0.5
SMGA3 (14.4km x 7.2km)	10	10	0.5
Nucleation Zone (4 km x 4km)	10	-10	0.2
Shallow Area	0	Depth-Dependent	2
Background Area	0	8	1

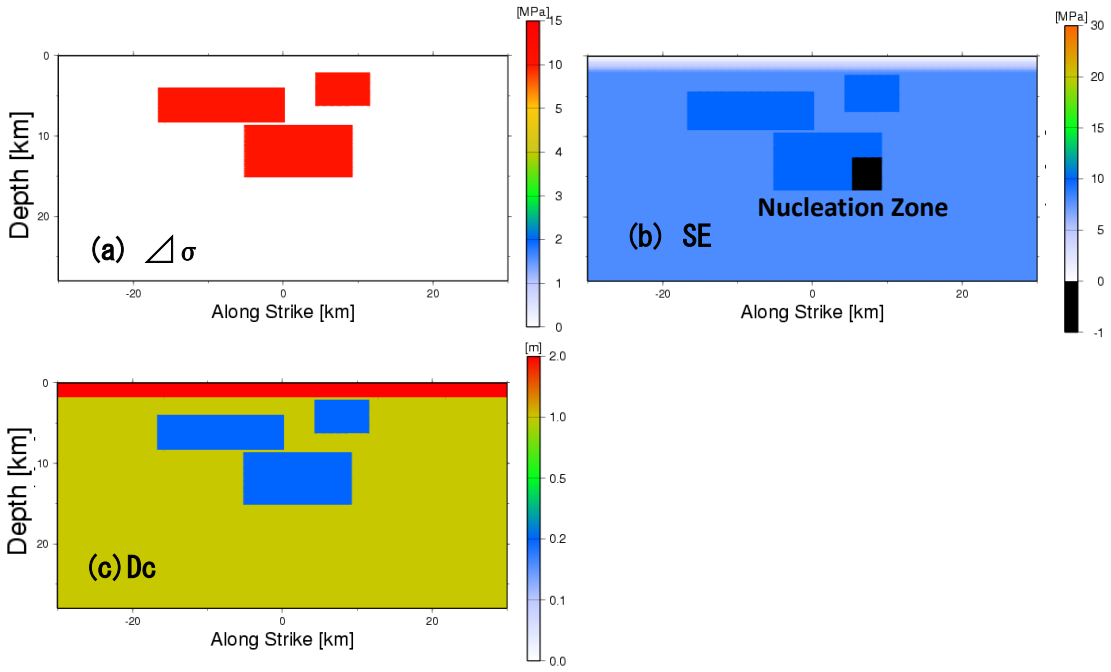

Fig. 4 Initial parameter distribution of the simulation (a)⊿σ, (b) SE, and (c) Dc

We have used the spectral-element method (SPECFEM3D, Galvez et al., [1], Komatitsch and Tromp, [16]) for the simulation. This method was originally developed to simulate seismic wave propagation at the global scale, and its numerical efficiency was improved by modification of the discretization formula of its shape functions. Also, the split-node parameterization of the fault plane (Dalguer and Day, [17]) has been incorporated into the dynamic model to simulate the source process.

3. Simulation Results

The simulated final slip distribution is shown in Fig. 5(a). The maximum simulated slip was 4.1 m, and the calculated seismic moment was 4.0e+19 [Nm] (Mw 7.0) if the area with final slip larger than 0.2 m (minimum Dc values) is defined as the fault area. The moment-rate function for the simulation had a relatively simple shape (Fig. 5(b)), suggesting that the source process resulting from this simulation was also simple. Fig 5(c) shows the contour map of the rupture time [s]. The rupture time is defined when the slip-rate function reaches to the 0.01 [m/s]. The rupture velocity around the shallow area is approximately around 2.0 km/s, consistent with the finite-fault inversion results [e.g., 6].

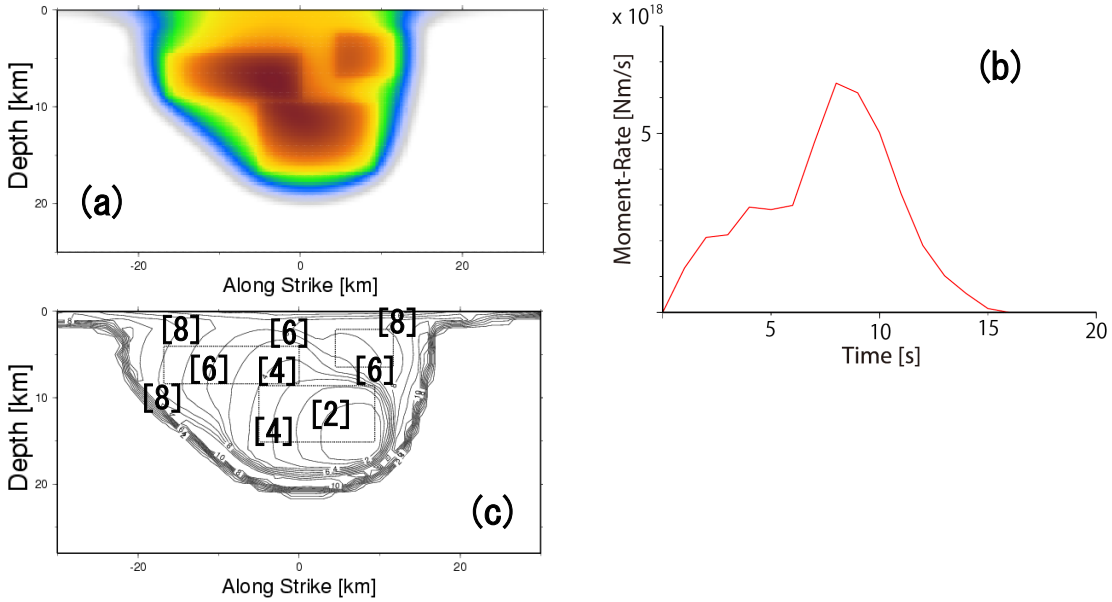

Fig. 5 (a) Final slip distribution, (b) moment-rate function and (c) contour map of the rupture time (sec), when slip rate reaches to 0.01 m/s. (The fault surface is defined as the area where the final slip is larger than 0.2m) Initial parameter distribution of the simulation.

We have shown the distribution of peak ground velocity (PGV) on the surface of the model for two horizontal components in Fig. 6. PGV value is calculated after the simulated ground motions were filtered lower than 1 [Hz]. The areas with large PGV values for the Fault-Normal component correspond to the edge of the large slip area projected to the surface. This trend is consistent with the dislocation problem for the strike slip fault. On the other hand, the area with large PGV values is relatively centered around the fault trace. We also plotted the location of the Nishihara village for both components. The observed records in Nishihara Village showed that the amplitude of Fault-parallel component is roughly two times larger than that of Fault-normal component (Fig. 1). The relationship between two horizontal components for our simulations agrees the observations.

We also compared the time histories of simulated ground motions on the points corresponding to the Nishihara village in Fig. 7. Due to the assumption of the homogeneous seismogenic material in the simulation, we corrected the amplitude based on the impedance ratio for the assumed with two layers. We

also adjusted the timing of the time histories with consideration to the staring time on the observation. Even the occurrence time and predominant frequency for the velocity pulses should be adjusted, the general trend of the amplitude has been reproduced. This suggests that our dynamic source model is working for reproducing the general features of velocity pulses. Also, this might suggest that the consideration of the detail features such as the nonplanar fault shape, heterogeneous material and consideration of Hinagu segment can develop the reproduction of observed records at Nishihara village.

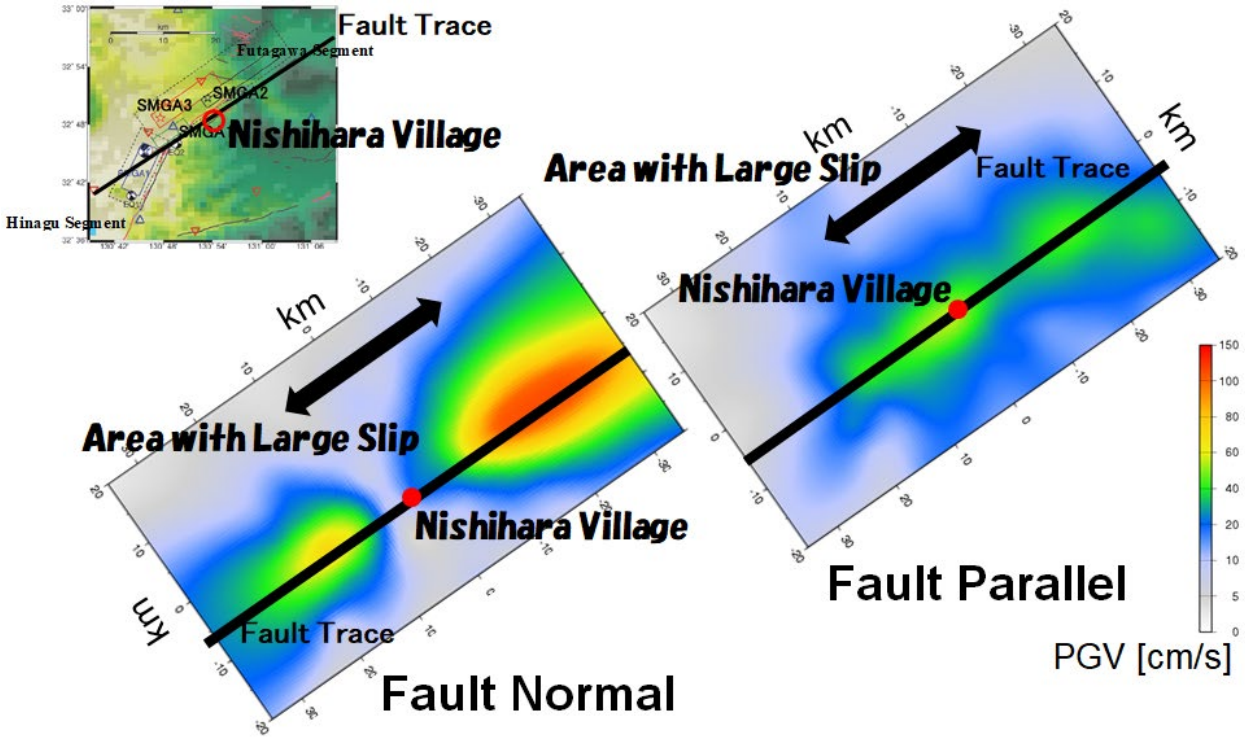

Fig. 6 Distibution of peak ground velocity for two horizaontal components on the suirface.The waves are filetered lower than 1 Hz when PGV is calcurated.

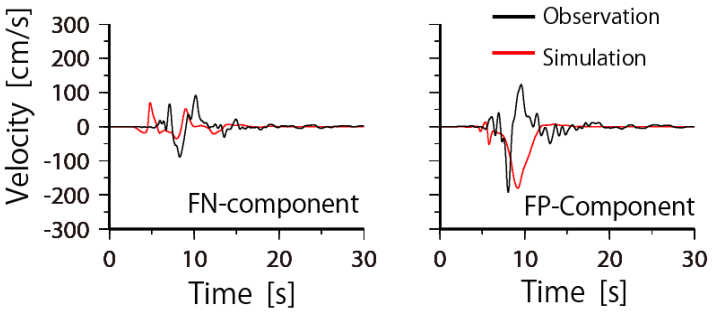

Fig. 7 Simulated ground motions at the Nishihsra Village with impedance correction. (Filetered lower than 1.0 Hz, strike is assumed to be 235N, Asano and Iwata [6])

4. Discussion

For the dynamic simulation, how the initial conditions can be set close to the real environment is one of the most important issues. In order to do it, the usage of the results from laboratory experiments have been

investigated, especially for the megathrust earthquakes (e.g., Tsuda *et al.,* [18]). They have succeeded to reproduce the basic features of the faulting behavior for the real earthquake (2011 Tohoku earthquake). However even the frictional parameters can be estimated via laboratory experiment, setting stress level is very difficult. For example, even the slip distributions can be reproduced based on the certain assumption of stress drop, the situation of reproduction of time histories is different. Here, we show how setting stress values can cause change in terms of ground motions, then make some discussions how such assumption is difficult to set "physically".

We have constructed the model with S=0.1 with reducing SE and keep stress drop same as the original model (S=1.0). The Fig 8(a) shows the final slip distibuition and (b) denotes the contour map of the rupture time for the model with S=0.1. As mentioned before, the model with same stress drop generated almost same final slip distributions as original model (S=1.0, Fig 5(a)) meaning that slip disribution is independent with S values.

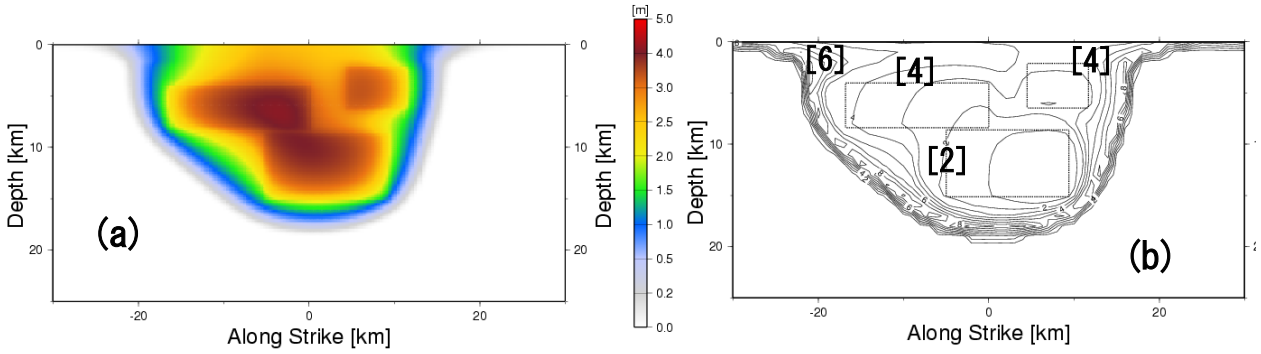

Fig. 8 (a) Final slip distribution (b) contour map of the rupture time (sec), when slip rate reaches to 0.01 m/s for S=0.1 model.

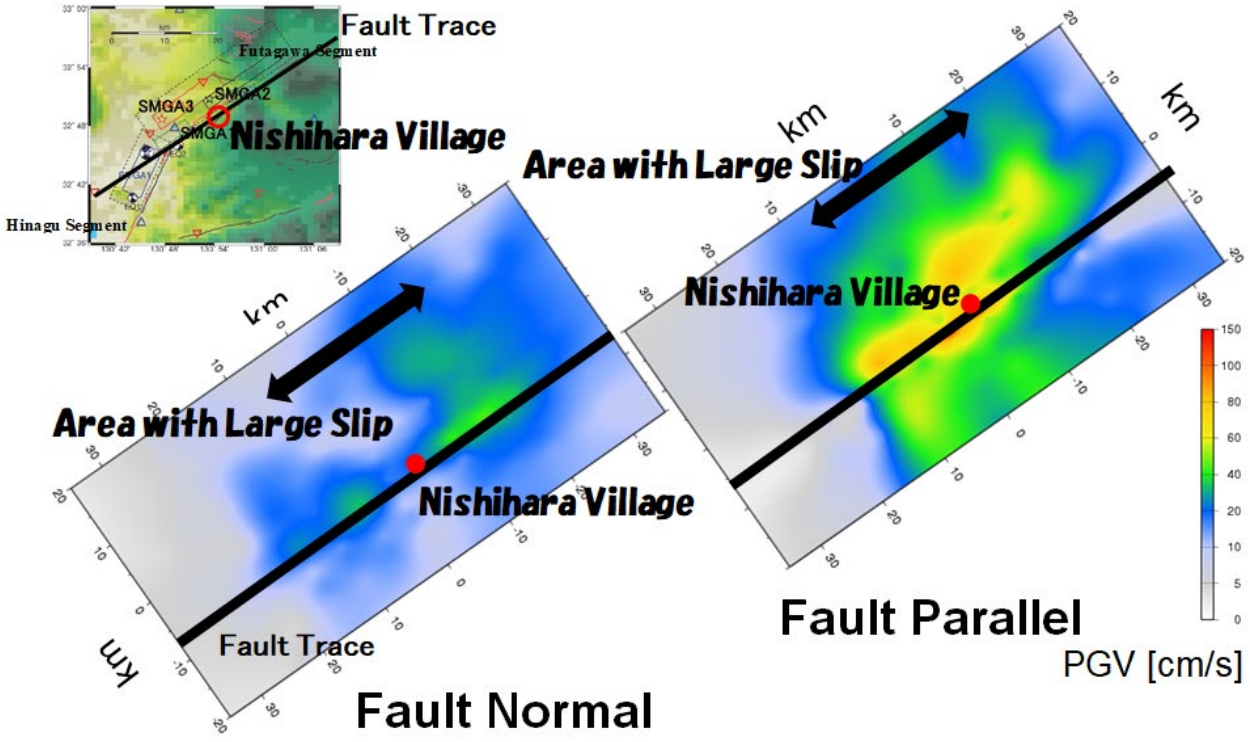

Fig. 9 Simulated ground motions at the Nishihsra Village with impedance correction.

On the other hand, the shape of the contour map of rupture time is completely different (Fig 5(c)). For the model with S=0.1, the rupture pripagates pretty fast and the rupture velocity exceeds S-wave velocity, showing super shear for the most part of the fault plane. This is completely agasint what the inversion results showed based on observed data. Also, Fig. 9 shows the distibutions of PGV from model with S=0.1. Even the area with large PGV values in Fault-pararrel component including the Nishihara village looks consistent with the observations, the situation shown in the rupture propagation (e.g., Fig 8(b)) denotes that such large values only reflect the initial conditions of the stress disribution, i.e., the fault plane is ruptured with very short amount of time.

Although Urata et al. [14] succeeded in reproducing the basic features of the source process of the Kumamoto earthquake using a dynamic model, they did not address the detailed ground motion features. Therefore, to simulate more physically plausible ground motions, more tuning of the model may be necessary to set appropriate values for the initial parameters such as the stress distribution and friction parameters.

5. Summary

In this study, we have applied the dynamic model to the ground motion simulation for the near-fault motions. The simulation is based on the spectral element method, which the modification of the formulation can lead to the more efficient calculation than conventional finite element method. We have assumed the three SMGA (Strong Motion Generation Area) on the fault plane referred to the model by previous studies. We explored the conditions of initial parameters, such as the location of SMGA, frictional parameters, stress parameters to investigate the conditions to generate the velocity pulses on the near fault motions, such as the observed records at the Nishihara Village during the 2016 Kumamoto Earthquake.

The agreement of the PGV values of simulation on the Nishihara village with the observed records suggested that the mechanism of generating velocity pulses might be investigated by the dynamic model even the occurrence time and predominant frequency for the velocity pulses should be adjusted. This indicates that the consideration of the detail features such as the nonplanar fault shape, heterogeneous material and consideration of Hinagu segment can develop the reproduction of observed records at Nishihara village.

Acknowledgement

We appreciate the discussion with Profs. J.P Ampuero and H. Kawabe to develop make forward this study.

6. References

[1] Galvez P, Ampuero, J. P., Dalguer, L. A., Somala, S. N., and Nissen-Meyer, T. F. (2014): Dynamic earthquake rupture modelled with an unstructured 3-D spectral element method applied to the 2011 M9 Tohoku earthquake. Geophysical Journal International, 198(2), 1222–1240.

[2] Satoh, T (2017): Broadband source characteristics of the 2016 Kumamoto earthquake estimated from strong motion records, J. Struct. Constr. Eng, Vol 82, 1707-1717. (In Japanese with English abstract)

[3] Koketsu, K (2018): *Physics of Seismic Ground Motion*. Kindai kagaku sha Co.,Ltd, Tokyo, Japan (In Japanese).

[4] Dunham, E. M. and R. J. Archuleta (2004): Evidence for a supershear transient during the 2002 Denali Fault earthquake, Bulletin of the Seismological Society of America, 94(6B), S256-S268, doi:10.1785/0120040616

[5] Ando, R. and Y. Kaneko (2018): Dynamic rupture simulation reproduces spontaneous multi-fault rupture and arrest during the 2016 Mw 7.9 Kaikoura earthquake, Geophys. Res. Lett, 45 (23), 12875-12883, 2018

[6] Asano K, and T. Iwata (2016): Source rupture processes of the foreshock and mainshock in the 2016 Kumamoto earthquake sequence estimated from the kinematic waveform inversion of strong motion data, Earth Planets Space, 68, 147, doi:10.1186/s40623-016-0519-9.

[7] Furumura, T (2016): Destructive near-fault strong ground motion from the 2016 Kumamoto prefecture, Japan, M7.3 earthquake, Landslides, V 13, Issue 6, pp 1519–1524.

[8] Yue, H., Ross, Z. E., Liang, C., Michel, S., Fattahi, and H., Fielding (2017): The 2016 Kumamoto Mw = 7.0 earthquake: A significant event in a fault–volcano system. Journal of Geophysical Research: Solid Earth, 122. doi.org/10.1002/2017JB014525

[9] Kobayashi, H., K. Koketsu, and H. Miyake (2017): Rupture processes of the 2016 Kumamoto earthquake sequence: Causes for extreme ground motions, Geophys. Res. Lett., 44, 6002-6010, doi:10.1002/2017GL073857

[10] Hikima K. (2016): Source rupture process of the 2016 Kumamoto earthquake and its foreshock estimated from strong motion waveforms, JAEE annual meeting 2016, P4-11. (in Japanese with English abstract)

[11] Tsuda, K. and H. Kawabe (2020): Development of A Method for Ground Motion Simulation based on the Physics-Based Model and its Application to the Near-Fault Motions, Hokudan International Symposium on Active Faulting 2020.

[12] Galis, M., Pelties, C., Kristek, J., Moczo, P., Ampuero, J. P., and Mai, P. M (2015): On the initiation of sustained slip-weakening ruptures by localized stresses. Geophysical Journal International, 200(2), 890–909

[13] Ida, Y (1972): Cohesive force across the tip of a longitudinal-shear crack and Griffith's specific surface energy. Journal Geophysical Research, 77, 3796–3805.

[14] Aochi H (2018): Dynamic asymmetry of normal and reverse faults due to constrained depth-dependent stress accumulation, Geophysical Journal International, Volume 215, 2134–2143, https://doi.org/10.1093/gji/ggy407

[15] Urata, Y., K. Yoshida, E. Fukuyama, and H. Kubo (2017): 3-D dynamic rupture simulations of the 2016 Kumamoto, Japan, earthquake, Earth Planets Space, 69, 150, doi: 10.1186/s40623-017-0733-0.

[16] Komatitsch, D., and J. Tromp (1999): Introduction to the spectral-element method for 3-D seismic wave propagation, Geophysical Journal International, vol. 139, p. 806-822.

[17] Dalguer, L. A., and S. M. Day (2007): Staggered-grid split-node method for spontaneous rupture simulation, J. Geophys. Res. , 112, B02302, doi:10.1029/2006JB004467

[18] Tsuda, K. J. Miyakoshi, Y. Imato, D. Sugiyama, S. Tsuboi (2019): Dynamic Rupture Simulations to Investigate the Behavior of Mega-Thrust Faults Constrained by Experimental Results, Journal of Association of Earthquake Engineering in Japan.(Japanese with English Abstract)

